lesion was served as 3D bio-paper. A long-wavelength UV exposure of maximum intensity 8.9mW/cm^2 at 365nm was set up for simultaneous photo-polymerization during printing. Printed cell-hydrogel constructs with OC plugs were cultured with ITS+ medium supplemented with 10 ng/mL TGFβ1 at 37°C with 5% CO_2. Samples were collected at 2, 4, 6 weeks for glycosaminoglycan (GAG)/DNA, collagen type II/DNA, gene expression, and histology analysis. Equilibrium swelling ratio and compressive modulus of printed PEGDMA hydrogels were measured and printed chondrocytes distribution within hydrogel was examined with confocal microscopy.

Results: Each printed layer (~0.3 μL) was instantly photo-polymerized during layer-by-layer deposition. Thus the delivered cells maintained their initially deposited 3D positions instead of sinking to the bottom due to gravity (Figure 1).

Equilibrium swelling ratio (6.19±0.10), water content (83.85±0.26%), and compressive modulus (395.73±80.40kPa) of printed PEG gel are within the range of the properties of native human articular cartilage. RT-PCR results showed reduced collagen type I expression and increased collagen type II as well as aggrecan during the culture. Collagen type II and aggrecan expression was significantly higher in chondrocytes printed to OC plug 3D bio-paper than that to mold. Gene expression data was confirmed with GAG/DNA and collagen type II/DNA analysis. Safranin O staining of hydrogel in OC plugs cultured for 2 weeks shows more proteoglycans production in the region contacting with the native cartilage.

Conclusions: Bio-printing based on thermal inkjet printing technology can be applied for precise 3D deposition of chondrocytes and biomaterial scaffold during layer-by-layer assembly. Direct cartilage repair is achieved by printing bio-ink *in situ* to cartilage defects with simultaneous photo-polymerization. Printed cell-hydrogel constructs are integrated to 3D bio-paper with induced chondrogenesis to the implanted cells. Therefore, bio-printing has the capacity to mimic native ECM distribution and cell organization for zonal cartilage tissue engineering. The interactions between native cartilage and printed materials can induce the chondrogenesis of implanted chondrocytes to deposit more ECM, which reveals the importance and possibility of developing *in vivo* bio-printing technology for direct cartilage repair.

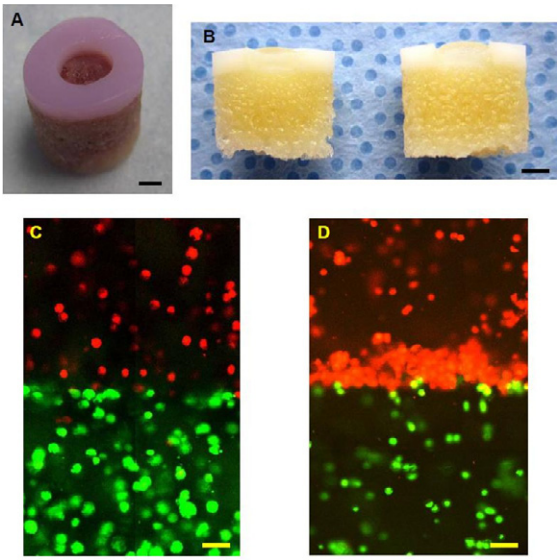

Fig. 1. Bovine OC plug (3D bio-paper) and distribution of printed human chondrocytes in PEG gel. (A) A 3D bio-paper with full thickness cartilage lesion; (B) 3D bio-paper cut in half after decalcification with printed hydrogel in the defect. (C) Printed cells remained deposited 3D positions with simultaneous photo-polymerization during layer-by-layer assembly. (D) Cells accumulated to the interface of the zonal structure due to gravity when polymerized after cell deposition. Scale bar: A,B 2 mm; C,D 100 μm.

93
IDENTIFICATION OF CHONDROGENIC PROGENITOR CELLS IN INJURED BOVINE ARTICULAR CARTILAGE

Y. Yu, D. Seol, D. McCabe, H. Zheng, J. Martin. *Univ. of Iowa, Iowas City, IA, USA*

Purpose: As an avascular and aneural tissue, articular cartilage has minimal healing ability and is often replaced by fibrous tissue after injury. Cell-based therapies for cartilage defects usually use chondrocytes for tissue engineering procedures. However, these cells rarely establish a hyaline cartilage matrix *in situ* and their harvest and implantation requires two operations. Our previous studies described a migratory progenitor-like cell (MP-like cell) population that appeared to reside within the superficial zone of bovine articular cartilage. These cells emerged in response to mechanical injury and migrated toward areas where chondrocytes were killed and the matrix was damaged. Moreover, MP-like cells were shown to be highly chondrogenic in vitro. These findings suggested that the cells might be capable of repairing cartilage lesions. The work presented here confirms that MP-like populations include cells with stem/progenitor cell characteristics as determined by side population (SP) discrimination assay using flow cytometry.

Methods: Injury Model: Bovine osteochondral explants were obtained from adult bovine knees. We subjected these explants to a single blunt impact blow (2.5 J/cm^2) via a 5 mm diameter platen using a drop tower device.

Isolation and culture of superficial chondrocytes: Five days after impact, explants were placed in trypsin for 20 minutes to harvest surface-migrating MP-like cells and in colagenase/pronase to harvest underlying normal chondrocytes. Cells were isolated and expanded in DMEM-based media for seven days.

Side population assay: The SP discrimination assay is based on the differential potential of cells to efflux the Hoechst dye via the ATP binding cassette (ABC) family of transporter proteins. Cells were trypsinized and counted for Hoechst dye staining in the presence of Verapamil, (inhibitor of ABC transporter). PI (Prodium Iodide) was used for dead cell discrimination. Normal chondrocytes were used as control.

Results: MP-like cells repopulated dead zones created by blunt impact injury (Figure 1). Side Populations were observed in both MP-like cells and normal chondrocytes (whole thickness), but with a significantly higher ratio within MP-like cells. Side population from MP cells was also much higher compared with bone marrow cells (BMSCs) and superficial zone cartilage (0.07%) (Figure 2).

Conclusions: Migrating cells found on the surfaces of injured osteochondral explants display stem/progenitor cell features. Their ability to home to injury sites and re-establish a hyaline-like extracellular matrix offers the potential for a new strategy for cartilage repair that requires minimal intervention.

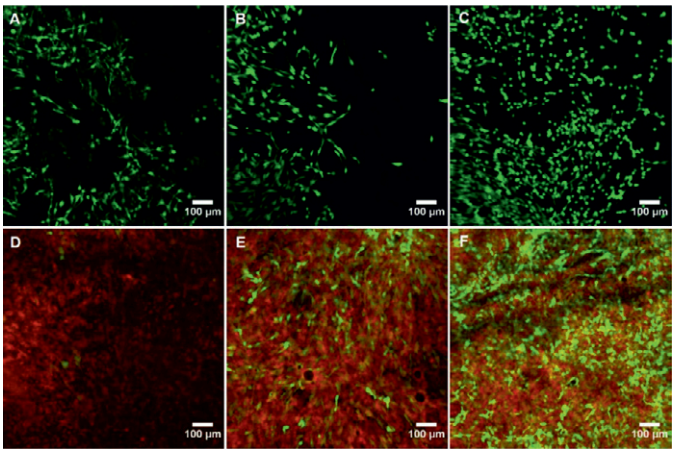

Fig. 1. Repopulation by progenitor-like cells in an impact injury site. (A-C) Calcein AM-stained cells (green) at the same site of an impact-injured explant. Elongated progenitor-like cells had migrated into the injury site at 7 days (A), 11 days (B), and 15 days (C) post-impact. (D-F) Migrated GFP-labeled progenitor-like cells (green) at the same site of a impact-injured explant. GFP-labeled cells implanted adjacent an impact area were migrated into the injured site at 2 days (D), 5 days (E), and 12 days (F) post-impact. Red: endogenous chondrocytes.

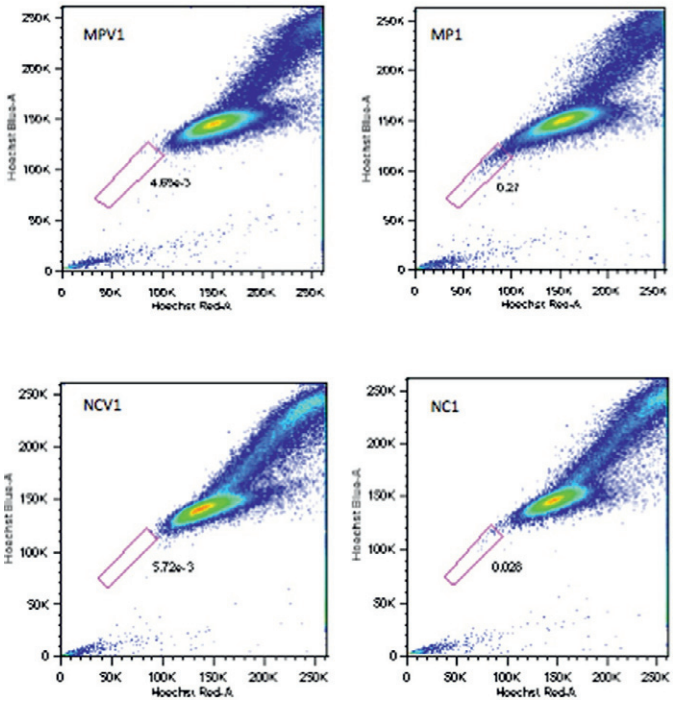

Fig. 2: Flow cytometry for SP assay with Hoechst dye concentration of 2.5 μ g/ml. Top: side population of MP-like cells, with the ratio of 0.27% (MP1). The side population is eliminated with verapamil (MPV1). Bottom: side population of normal chondrocytes, with the ratio of 0.028%.

94
RELATIONSHIP BETWEEN HIP ADDUCTION MOMENT, HIP ABDUCTOR STRENGTH AND PROGRESSION OF KNEE OSTEOARTHRITIS

C.O. Kean, K.L. Bennell, K. Bowles, R.S. Hinman. *Univ. of Melbourne, Melbourne, Australia*

Purpose: Previous research had found that an increased hip adduction moment during walking was protective of knee osteoarthritis (OA) progression (based on radiographic medial joint space grading). It is speculated that this is due to stronger hip abductor muscles which help stabilize the pelvis on the stance limb and prevent pelvic drop of the swing limb. If the hip abductors of the stance limb are weak, the pelvis may drop towards the contralateral swing limb resulting in a shift of the centre of mass away from the stance limb, thereby increasing the frontal plane lever arm at the knee and subsequently increasing the peak knee adduction moment, a proxy for medial compartment loading. The purposes of this study were to examine the relationship between baseline a) hip adduction moment and b) hip abductor strength, and changes in cartilage morphology over 12 months in people with medial knee OA.

Methods: 200 individuals with medial knee OA were recruited for a clinical trial evaluating the efficacy of lateral wedge insoles on slowing structural disease progression. Since the wedges had no effect on symptoms or structural changes, data from 144 participants (71 lateral wedge insoles, 73 control insoles; 72% of participants) who completed a three-dimensional gait analysis, as well as baseline and follow-up MRIs, were pooled for the current study. A subset of participants from the control insoles group (n = 49) also underwent hip abductor strength testing at baseline. Sagittal MR knee images were obtained on a 1.5-T whole body unit. Annual change in tibial cartilage volume was determined by subtracting the follow-up volume from baseline volume and dividing by time between scans. Progression of cartilage defects and bone marrow lesions (BMLs) was determined by subtracting the cartilage defect/BML grade at follow-up from that at baseline. A value less than or equal to −1 represented progression. A multiple linear regression model was used to examine the relationship between hip adduction moment (independent variable) and annual change in medial tibial cartilage volume (dependent variable). Binary logistic regressions were used to examine the association between hip adduction moment (independent variable) and progression of tibiofemoral cartilage defects and BMLs (dichotomized dependent variables). Analyses were repeated using hip abductor strength as the independent variable. All models were initially adjusted for age, sex, body mass index and repeated with additional covariates of intervention group, MRI machine and alignment.

Results: Baseline hip adduction moment during walking and hip abductor strength were not associated with either change in medial tibial cartilage volume or progression of medial tibiofemoral cartilage defects or BMLs (Table 1).

Table 1. Relationship between hip adduction moment, abductor strength and change in cartilage

	Univariate analysis		Multivariate analysis*		Multivariate analysis**	
	Regression coefficient (95% CI)	P value	Regression coefficient (95% CI)	P value	Regression coefficient (95% CI)	P value
Annual change medial tibial cartilage volume						
Peak hip adduction moment (%BW*ht)	2.26 (−3.26, 7.77)	0.42	3.95 (−2.92, 10.82)	0.26	3.78 (−3.15, 10.72)	0.29
Hip abduction strength (Nm/kg)	3.79 (−32.53, 40.10)	0.84	8.57 (−32.75, 49.89)	0.68	0.68 (−41.56, 42.95)	0.97
	Odds ratio (95% CI)	P value	Odds ratio (95% CI)	P value	Odds ratio (95% CI)	P value
Progression of Medial Tibiofemoral Cartilage Defects (yes/no)						
Peak hip adduction moment (%BW*ht)	1.08 (0.84, 1.39)	0.55	1.09 (0.79, 1.49)	0.36	1.09 (0.79, 1.51)	0.60
Hip abduction strength (Nm/kg)	1.27 (0.09, 2.54)	0.78	0.72 (0.13, 4.14)	0.72	0.73 (0.13, 4.28)	0.73
Progression of Medial Tibiofemoral BMLs (yes/no)						
Peak hip adduction moment (%BW*ht)	0.91 (0.72, 1.16)	0.46	0.93 (0.69, 1.25)	0.63	0.93 (0.69, 1.26)	0.64
Hip abduction strength (Nm/kg)	0.01 (0.01, 1.55)	0.10	0.07 (0.00, 1.4)	0.08	0.06 (0.00, 1.33)	0.08

95% CI = 95% confidence interval.
*adjusting for age, gender, body mass index.
** adjusting for age, gender, body mass index, intervention group, MRI machine and alignment.

Conclusions: These findings suggest that neither an increased hip adduction moment nor increased hip abductor strength is protective against change in cartilage volume/morphology in medial knee OA. These findings are consistent with recent hip strengthening intervention studies which have found that increased hip abductor strength does not alter the knee adduction moment.

95
KNEE ALIGNMENT MAY INFLUENCE PERI-ARTICULAR BONE MORPHOLOGY

G.H. Lo[1,2], T.E. McAlindon[3]. *[1]Michael E. DeBakey Dept. of Veteran's Affairs Med. Ctr., Houston, TX, USA; [2]Baylor Coll. of Med., Houston, TX, USA; [3]Tufts Med. Ctr., Boston, MA, USA*

Purpose: Static alignment influences loading in the knee joint and is a potent predictor of disease progression in those with osteoarthritis (OA). The peri-articular bone has a major role in force dispersion across the knee and changes in its structure, both adaptive and pathological, are prominent in OA. However, the interplay between knee biomechanics and the state of the peri-articular bone is not fully understood. Our objective was to evaluate the influence of static knee joint alignment on peri-articular trabecular morphology measured by MRI and on bone mineral density (BMD) using dual x-ray absorptiometry (DXA).

Methods: This was a cross-sectional analysis of 320 enrollees into the Osteoarthritis Initiative (OAI) Bone Ancillary Study, who received trabecular MRI and peri-articular bone mineral density (paBMD) measurements of one knee at the Ancillary baseline visit (parent study 30 or 36 month visits) who also had comprehensive physical exams at the parent study 24 month visits that included goniometric evaluation of static alignment, where negative values were valgus and positive varus. A correction factor was applied to the physical exam static alignment measures to more closely represent mechanical alignment. Knee and femoral neck DXAs were obtained using GE Lunar Prodigy DXA scanners at the Ancillary baseline. Knee DXAs were used to measure an absolute medial tibial peri-articular bone mineral density (paBMD) and a medial:lateral tibial paBMD ratio.

Trabecular morphometry MRIs were also obtained at Ancillary baseline using 3T MRIs. The medial tibial periarticular bone was analyzed using a customized software package (calcDCN) to provide measures of total bone volume fraction (tBVF), trabecular number, spacing and thickness (Tb.N, Tb.Sp, and Tb.Th).

We performed Pearson's correlations to evaluate associations of static alignment with trabecular morphometry measures, paBMD, medial:lateral tibial paBMD ratio, femoral neck BMD, age, and body mass index (BMI). We also performed subgroup analyses among those without and with radiographic evidence of OA (Kellgren/Lawrence grade <2 v. ≥2).